

Anisotropic nonlinear response of silicon in the near-infrared region

J. Zhang

Department of Electrical and Computer Engineering, University of Rochester, New York 14627

Q. Lin,^{a)} G. Piredda, R. W. Boyd, and G. P. Agrawal

Institute of Optics, University of Rochester, Rochester, New York 14627

P. M. Fauchet

Department of Electrical and Computer Engineering and Institute of Optics, University of Rochester, New York 14627

(Received 15 June 2007; accepted 13 July 2007; published online 15 August 2007)

The authors characterize experimentally the anisotropy of two-photon absorption and the Kerr nonlinearity in silicon over a broad spectral region in the near infrared using the z -scan technique. The results show that both of these parameters decrease by about 12% along the $[0\ 1\ 0]$ direction compared with the $[0\ 1\ \bar{1}]$ direction, and this change occurs for wavelengths in the range of 1.2–2.4 μm . © 2007 American Institute of Physics. [DOI: 10.1063/1.2768632]

Silicon photonics is emerging as a new branch of optics because of its potential applications in the near- and mid-infrared regions.^{1,2} Silicon-on-insulator (SOI) waveguides can confine optical modes tightly to a narrow region, providing an excellent platform for realizing optical functions on a submicron scale by exploiting a multitude of nonlinear effects. Although silicon lacks a second-order nonlinear susceptibility because of its centrosymmetric crystal structure, it exhibits a relatively large third-order susceptibility $\chi^{(3)}$ with a magnitude nearly 200 times larger than that of silica. Indeed, SOI waveguides have recently been used for multiple nonlinear applications, and they are a likely candidate for future all-optical signal processing at the chip level.^{3–10}

Polarization effects play an important role inside SOI waveguides in both the linear and nonlinear regimes.^{11–13} Unlike the isotropic nature of linear optical properties of silicon, its third-order nonlinear response is generally anisotropic because of the point-group symmetry of a silicon crystal. As SOI waveguides are typically fabricated along the $[0\ 1\ 1]$ direction on the $(1\ 0\ 0)$ surface, the commonly used quasi-TM and quasi-TE modes are polarized along the $[1\ 0\ 0]$ and $[0\ 1\ \bar{1}]$ directions, respectively.^{4–6,8,10,12} Consequently, any anisotropy of silicon nonlinearity affects the nonlinear processes, depending on the polarization of the input light. For example, anisotropy in the Raman tensor of silicon has been shown to play a crucial role in Raman amplification and lasing.^{5,6} It is thus important to know the exact magnitude of the $\chi^{(3)}$ anisotropy, particularly as is related to the two important nonlinear parameters known as the two-photon absorption (TPA) and the Kerr coefficients, both of which play a critical role in silicon-based devices.^{3–10}

The $\chi^{(3)}$ anisotropy of silicon has been studied in the past four decades mainly through third-harmonic generation and four-wave mixing.^{14–20} However, most studies have focused on the opaque spectral regime, well above the indirect band gap (near 1.1 μm), to explore the complicated relationship between $\chi^{(3)}$ and the band structure of silicon. In the case of nonlinear silicon photonics, one is more interested in the region below the indirect band gap, where silicon is

transparent.^{1,2} However, little information is available about the anisotropy of $\chi^{(3)}$ in the region between 1.2 and 2.4 μm , where the nonlinearity is expected to be dispersive.^{21–24} In this letter, we present a detailed characterization of the $\chi^{(3)}$ anisotropy over this broad spectral region. Although third-harmonic generation provides high sensitivity, it involves interacting waves of quite different frequencies and is thus affected by the dispersion of $\chi^{(3)}$. To exclude such undesirable effects, we employ a simple method based on the z -scan technique.²⁵ This method depends on the nonlinear absorption and self-focusing induced by only one optical wave and still provides relatively high measurement sensitivity.²⁶

As a silicon crystal belongs to the $m3m$ point-symmetry group, its $\chi^{(3)}$ has only two independent components, namely, $\chi_{1111}^{(3)}$ and $\chi_{1122}^{(3)}$.²⁷ For a linearly polarized wave incident normally on the $(1\ 0\ 0)$ surface of a silicon wafer, the induced nonlinear polarization is given by²⁷

$$P_i^{(3)} = \frac{3\epsilon_0}{4} [\chi_{1111}^{(3)} |E_i|^2 E_i + \chi_{1122}^{(3)} (2|E_j|^2 E_i + E_i^* E_j^2)], \quad (1)$$

where E_i and E_j ($i, j = x, y$ with $i \neq j$) are the two polarization components along the in-plane crystallographic axes x and y pointing toward $[0\ 1\ 0]$ and $[0\ 0\ 1]$ directions, respectively. Although the polarization in Eq. (1) would introduce a slight nonlinear polarization rotation on the optical beam (because of slightly different nonlinear phases imposed on the two polarization components), a detailed analysis shows that the TPA and self-focusing effects in a z -scan experiment are primarily dominated by the component of $P^{(3)}$ that is copolarized with the input beam. As a result, the nonlinear effects can be described by an effective susceptibility of the form²⁵

$$\chi_{\text{eff}}^{(3)}(\theta) = \frac{1}{4} [A + B \cos(4\theta)], \quad (2)$$

where $A \equiv 3\chi_{1111}^{(3)} + 3\chi_{1122}^{(3)}$, $B \equiv \chi_{1111}^{(3)} - 3\chi_{1122}^{(3)}$, and θ is the incident polarization angle with respect to a crystallographic axis, chosen to be the x axis.

In a z -scan experiment, the beam transmittance in the cases of open and partially closed apertures is governed by²⁶

$$T_o(z, \theta) = 1 - \frac{\beta_T(\theta) I_0 L}{2\sqrt{2}(1 + \eta^2)}, \quad (3)$$

^{a)}Electronic mail: linq@optics.rochester.edu

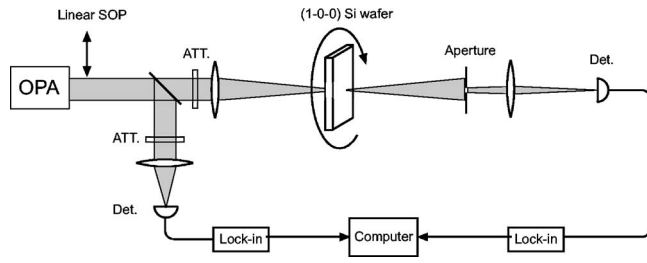


FIG. 1. Experimental setup used for the measurements of anisotropy. OPA: optical parametric amplifier; ATT: attenuator; Det: detector; and SOP: state of polarization.

$$T_c(z, \theta) = 1 - \frac{I_0 L [\beta_T(\theta) D_r - 2kn_2(\theta) D_i]}{2\sqrt{2}S(1 + \eta^2)}, \quad (4)$$

where I_0 is the peak intensity of the incident beam, L is the thickness of the sample, and $\eta \equiv z/z_0$ is the location of the sample with respect to the focal point, normalized by the Rayleigh range ($z_0 = \pi w_0^2/\lambda$), of a focused Gaussian beam with the waist radius w_0 at wavelength λ . $k = 2\pi/\lambda$ is the propagation constant in vacuum. Further, S is the aperture transmittance and D_r and D_i are quantities related to the filtered beam profile, given by:²⁴

$$D_r + iD_i = 1 - \exp\left[\frac{2(\eta - i)(\eta + 3i)}{\eta^2 + 9} \ln(1 - S)\right]. \quad (5)$$

In Eqs. (3) and (4), $\beta_T(\theta)$ and $n_2(\theta)$ are the TPA and Kerr coefficients for an input wave polarized linearly at an angle of θ with respect to the x axis. They are related to the effective third-order susceptibility in Eq. (2) as

$$kn_2(\theta) + \frac{i}{2}\beta_T(\theta) = \frac{3k}{4\epsilon_0 c n^2} \chi_{\text{eff}}^{(3)}(\theta), \quad (6)$$

where n is the polarization-independent refractive index of silicon.

Equations (2)–(6) provide a simple way to measure the anisotropy of n_2 and β_T . For example, Eq. (3) shows that the open-aperture trace exhibits an absorption dip in linearly proportion to the TPA coefficient β_T . Thus, by locating the sample at the focal point while changing the polarization angle θ , and comparing the data with those recorded far from the focal point, we can obtain the relative magnitude of $\beta_T(\theta)$ as a function of θ . Similarly, as D_r and D_i are even and odd functions of z , respectively [see Eq. (5)], the fractional transmittance $T_d(z, \theta) \equiv T_c(z, \theta)/T_o(z, \theta)$ exhibits a peak and a valley located symmetrically around the focal point. The difference in T_d at these two locations, denoted by $D_{pv}(\theta)$, is linearly proportional to the Kerr coefficient $n_2(\theta)$.²⁵ Therefore, by measuring $D_{pv}(\theta)$ as a function of polarization angle, we can obtain the relative magnitude of $n_2(\theta)$. In practice, it suffices to measure the difference of $T_c(z, \theta)$ at these two locations, as $T_o(z, \theta)$ has the same value at these two locations. Moreover, as only the relative magnitudes of β_T and n_2 are being characterized, this method does not require accurate information about the beam waist, peak intensity, etc., as long as these quantities remain stable during the measurement. As a result, the method has a much higher accuracy than those measuring absolute values of nonlinear parameters.²⁵

Figure 1 shows our experimental setup. 500-Hz linearly polarized optical pulses from an optical parametric amplifier

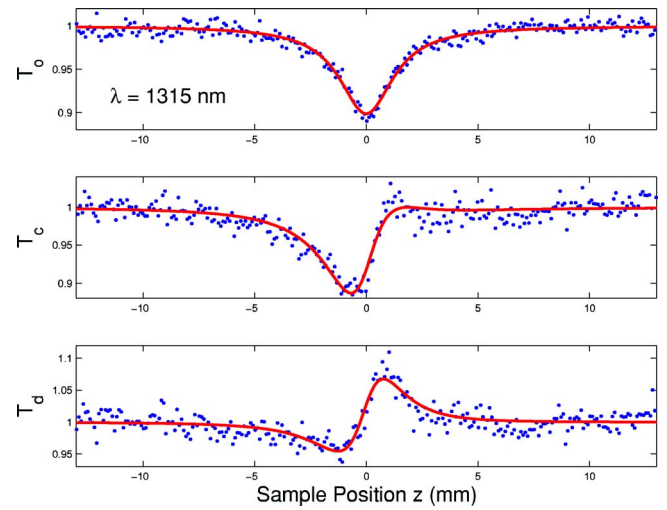


FIG. 2. (Color online) z -scan traces at 1315 nm with a pulse energy of 13 nJ (corresponding peak intensity of 10.0 GW/cm²). Top: open-aperture trace $T_o(z)$; middle: close-aperture trace $T_c(z)$ with the aperture transmittance $S = 0.5$; and bottom: $T_d(z) = T_c(z)/T_o(z)$. Blue dots and red curves show experimental data and theoretical fits, respectively. The incident wave is polarized along [010] direction.

(Spectra Physics, OPA-800FC) are focused onto a 500- μm -thick silicon wafer (p doped with a resistivity of 20 Ω cm) using a 10 cm focal-length lens. The wavelength is tunable from 1.2 and 2.4 μm , enabling us to measure the $\chi^{(3)}$ anisotropy over such a broad spectral region. The pulse width varies in the range of 90–150 fs, depending on the wavelength, and is short enough to ensure small free-carrier effects over the pulse duration. A small portion of the signal is used as a reference beam to monitor pulse energy fluctuations. The signal channel is divided by the reference one to mitigate the impact of such fluctuations. The (1 0 0) wafer under test is oriented such that the signal is normally incident along the [1 0 0] direction. For experimental simplicity, the polarization angle θ is varied by rotating the sample around its normal axis, the [1 0 0] direction.

We perform both the open- and close-aperture z scans and divide the two traces to obtain $T_d(z) = T_c(z)/T_o(z)$. Figure 2 shows the three traces at the carrier wavelength of 1315 nm. The T_o trace shows a clear TPA dip at a certain location z_d , while a peak and a valley appear in $T_d(z)$ because of self-focusing at locations denoted by z_p and z_v . At these three locations, we record T_o and T_c as a function of the sample orientation angle θ . We also record $T_o(\infty, \theta)$ and $T_c(\infty, \theta)$ with the sample far from the focal point, where both the TPA and self-focusing are negligible, to ensure the absence of other polarization-dependent effects. As discussed earlier, the quantities $T_o(z_d, \theta) - T_o(\infty, \theta)$ and $T_c(z_p, \theta) - T_c(z_v, \theta)$ provide a direct measure of the polarization dependence of the TPA coefficient $\beta_T(\theta)$ and the Kerr coefficient $n_2(\theta)$, which in turn are related to the imaginary and real parts of $\chi_{\text{eff}}^{(3)}$.

Figure 3 shows the normalized $\beta_T(\theta)$ and $n_2(\theta)$ as a function of the sample orientation angle θ . Both curves exhibit sinusoidal oscillations with a period of 90° because of the symmetry of silicon crystal, as indicated in Eq. (2). These oscillation patterns indicate clearly the polarization-dependent nature of the third-order nonlinearity in silicon. The minimum and maximum values of $\beta_T(\theta)$ and $n_2(\theta)$ occur when the sample is oriented at 0° and 45°, respectively,

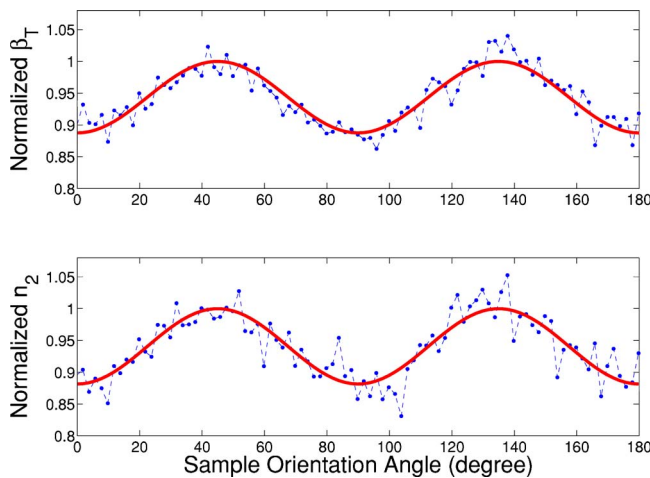


FIG. 3. (Color online) Normalized TPA coefficient β_T and Kerr coefficient n_2 as a function of sample orientation angle θ . Blue dots show the experimental data; red curve is a sinusoidal fit; and $\theta=0$ corresponds to a beam linearly polarized along the $[0\ 1\ 0]$ direction.

corresponding to the linear polarization along the $[0\ 1\ 0]$ and $[0\ 1\ \bar{1}]$ directions. The minimum value is about 88% of the maximum value for both β_T and n_2 . Our measurements made in the bulk material imply that the fundamental quasi-TM mode experiences about 12% less nonlinearity than the fundamental quasi-TE mode in conventional SOI waveguides. We stress that the two polarization directions used in the experiment coincide with the TE- and TM-mode directions in such waveguides because they are typically fabricated along the $[0\ 1\ 1]$ direction on the $(1\ 0\ 0)$ surface (and the longitudinal component along the propagation direction contains a very small fraction of the incident power). The uncertainty in our measurement mainly comes from slow fluctuations in pulse energy during measurements.

We can use the preceding results to deduce the anisotropy of $\chi^{(3)}$ itself. Equation (2) shows that $\chi_{\text{eff}}^{(3)}(0) = \chi_{1111}^{(3)}$ and $\chi_{\text{eff}}^{(3)}(45^\circ) = (\chi_{1111}^{(3)} + 3\chi_{1122}^{(3)})/2$. As $\beta_T(\theta)$ and $n_2(\theta)$ in Fig. 3 have a nearly the same polarization dependence, we obtain $\chi_{1111}^{(3)}/\chi_{1122}^{(3)} = 2.36$. This value is very close to the value measured at a wavelength of $1.06\ \mu\text{m}$, a value right above the indirect band gap,^{15,17,18} and indicates negligible dispersion in the anisotropy in this spectral region. As the absolute magnitudes of β_T and n_2 are quite dispersive from the full band gap to below half band gap,^{23,24} we vary the carrier wavelength of pulses from 1.2 to $2.4\ \mu\text{m}$ and characterize the anisotropy over this range. We find nearly the same magnitude of nonlinearity anisotropy over this near-infrared spectral region. Our results differ from recent experiments^{28,29} based on TPA in a silicon detector at $1550\ \text{nm}$, where the induced photocurrent was found to be polarization independent. This opens an interesting question about the fundamental physical relationship between silicon TPA and induced photocurrent. Further experimental and theoretical investigations are needed to clarify this issue.

In summary, we have carried out a detailed characterization of the anisotropy of the TPA and Kerr coefficients of silicon over a broad spectral range in the near infrared using

the z -scan technique. Our results show that both of these parameters decrease by about 12% along the $[0\ 1\ 0]$ direction compared with the $[0\ 1\ \bar{1}]$ direction, and this change occurs for wavelengths in the range of 1.2 – $2.4\ \mu\text{m}$. Based on these results, we find that the two independent components of the third-order susceptibility of silicon have the ratio of $\chi_{1111}^{(3)}/\chi_{1122}^{(3)} \approx 2.36$ over the broad wavelength range of our measurements. The discrepancy between our direct optical measurements and those obtained from TPA-induced photocurrent in a silicon detector raises an interesting fundamental question regarding the relationship between the nonlinear optical properties and electronic response of silicon.

This work is supported in part by AFOSR.

- ¹R. Soref, IEEE J. Sel. Top. Quantum Electron. **12**, 1678 (2006).
- ²R. A. Soref, S. J. Emelett, and W. R. Buchwald, J. Opt. A, Pure Appl. Opt. **8**, 840 (2006).
- ³V. R. Almeida, C. A. Barrios, R. R. Panepucci, and M. Lipson, Nature (London) **431**, 1081 (2004).
- ⁴H. Rong, A. Liu, R. Jones, O. Cohen, D. Hak, R. Nicolaescu, A. Fang, and M. Paniccia, Nature (London) **433**, 292 (2005).
- ⁵A. Liu, H. Rong, R. Jones, O. Cohen, D. Hak, and M. Paniccia, J. Lightwave Technol. **24**, 1440 (2006).
- ⁶B. Jalali, V. Raghunathan, D. Dimitropoulos, and Ö. Boyraz, IEEE J. Sel. Top. Quantum Electron. **12**, 412 (2006).
- ⁷H. Fukuda, K. Yamada, T. Shoji, M. Takahashi, T. Tsuchizawa, T. Watanabe, J. Takahashi, and S. Itabashi, Opt. Express **13**, 4629 (2005).
- ⁸H. Rong, Y. Kuo, A. Liu, M. Paniccia, and O. Cohen, Opt. Express **14**, 1182 (2006).
- ⁹M. A. Foster, A. C. Turner, J. E. Sharping, B. S. Schmidt, M. Lipson, and A. L. Gaeta, Nature (London) **441**, 960 (2006).
- ¹⁰I. Hsieh, X. Chen, J. I. Dadap, N. C. Panoiu, R. M. Osgood, Jr., S. J. McNab, and Y. A. Vlasov, Opt. Express **15**, 1135 (2007).
- ¹¹G. Reed, G. Mashanovich, W. Headley, B. Timotijevic, F. Gardes, S. Chan, P. Waugh, N. Emerson, C. Png, M. Paniccia, A. Liu, D. Hak, and V. Passaro, IEEE J. Sel. Top. Quantum Electron. **12**, 1335 (2006).
- ¹²V. Raghunathan, R. Claps, D. Dimitropoulos, and B. Jalali, J. Lightwave Technol. **23**, 2094 (2005).
- ¹³Q. Lin, J. Zhang, P. M. Fauchet, and G. P. Agrawal, Opt. Express **14**, 4786 (2006).
- ¹⁴J. J. Wynne, Phys. Rev. **178**, 1295 (1969).
- ¹⁵W. K. Burns and N. Bloembergen, Phys. Rev. B **4**, 3437 (1971).
- ¹⁶D. J. Moss, H. M. van Driel, and J. E. Sipe, Appl. Phys. Lett. **48**, 1150 (1986).
- ¹⁷C. C. Wang, J. Bomback, W. T. Donlon, C. R. Huo, and J. V. James, Phys. Rev. Lett. **57**, 1647 (1986).
- ¹⁸D. J. Moss, H. M. van Driel, and J. E. Sipe, Opt. Lett. **14**, 57 (1989).
- ¹⁹D. J. Moss, E. Ghahramani, J. E. Sipe, and H. M. van Driel, Phys. Rev. B **41**, 1542 (1990).
- ²⁰R. Buhleier, G. Lüpke, G. Marowsky, Z. Gogolak, and J. Kuhl, Phys. Rev. B **50**, 2425 (1994).
- ²¹M. Dinu, F. Quochi, and H. Garcia, Appl. Phys. Lett. **82**, 2954 (2003).
- ²²V. Raghunathan, R. Shori, O. M. Stafsudd, B. Jalali, Phys. Status Solidi A **203**, R38 (2006).
- ²³A. D. Bristow, N. Rotenberg, and H. M. van Driel, Appl. Phys. Lett. **90**, 191104 (2007).
- ²⁴Q. Lin, J. Zhang, G. Piredda, R. W. Boyd, P. M. Fauchet, and G. P. Agrawal, Appl. Phys. Lett. **91**, 021111 (2007).
- ²⁵R. DeSalvo, M. Sheik-Bahae, A. A. Said, D. J. Hagan, and E. W. Van Stryland, Opt. Lett. **18**, 194 (1993).
- ²⁶M. Sheik-Bahae, A. A. Said, T. Wei, D. J. Hagan, and E. W. Van Stryland, IEEE J. Quantum Electron. **26**, 760 (1990).
- ²⁷P. D. Maker and R. W. Terhune, Phys. Rev. **137**, A801 (1965).
- ²⁸R. Salem and T. E. Murphy, Opt. Lett. **29**, 1524 (2004).
- ²⁹T. Kagawa and S. Ooami, Jpn. J. Appl. Phys., Part 1 **46**, 664 (2007).